

Compact chirped-pulse amplification systems based on highly Tm³⁺ doped germanate fiber

ZHENGQI REN,¹ FEDIA BEN SLIMEN,^{1,*} JORIS LOUSTEAU,² NICHOLAS WHITE,¹
YONGMIN JUNG,¹ JONATHAN H. V. PRICE,¹ DAVID J. RICHARDSON,¹ FRANCESCO
POLETTI¹

¹Optoelectronics Research Centre, University of Southampton, SO17 1BJ, UK

²Department of Chemistry and Materials Engineering (CMIC), Politecnico di Milano, Via Mancinelli, 7, 20131 Milano, Italy

*Corresponding author: f.ben-slimen@soton.ac.uk

Received XX Month XXXX; revised XX Month, XXXX; accepted XX Month XXXX; posted XX Month XXXX (Doc. ID XXXXX); published XX Month XXXX

We report the fabrication of a dual cladding large mode area (LMA) thulium doped germanate fiber (TDGF). The fiber has a core diameter of 20 μm, a high Tm³⁺ ion concentration of 3×10²⁰/cm³ and an hexagonal inner-cladding to enhance pump absorption when cladding pumped. [Using short length of it, we demonstrate a compact 300 fs chirped-pulse amplification \(CPA\) system operating at 1925 nm, investigating both core- and cladding-pumped implementations.](#) By cladding pumping a 65 cm length we produced an average power of 14.1 W (limited by thermally induced damage) and a peak-power of 2.17 MW at a pulse repetition rate of 15.7 MHz. Core pumping a 19 cm length of TDGF produced 2.3 W of average power and 16 MW peak-power pulses at 0.39 MHz. The performance is already comparable to the state of the art achieved with flexible silica fibers. Considering the rapid improvements in glass quality and the scope for further increasing the doping concentration, this fiber type holds great potential for pulsed fiber lasers in the 1.5-3 μm wavelength region. © 2020 Optical Society of America

<http://dx.doi.org/10.1364/OL.99.099999>

High power ultra-short pulse laser sources in the 2 μm wavelength range are gaining more and more attention for use in applications including free space optical communications, sensing, material processing and mid-IR generation [1]. They are also proving promising for fundamental research in fields such as high harmonic generation [2] and laser-driven electron acceleration [3]. [Thulium \(Tm\)-doped photonic crystal fibers \[4,5\] have been used to achieve the highest pulse energies \(mJ level\), peak/average powers \(GW/kW\) to date.](#) However, many important practical applications, including material processing and power scaling of mid-IR light generation, do not require such levels of performance and consequently there is appreciable commercial interest in more

practical, compact sources based around more conventional flexible fiber technology with relatively simple physical configurations.

The current performance records for compact, high power Tm-based ultrafast fiber laser systems have been set by using conventional silica fibers. For example, Wan et al. demonstrated a CPA system, which achieved an output average power of 32 W by using 650 meters of fiber stretcher and 4.5 m LMA fiber [6]. The generation of 0.15 μJ energy, 0.5 MW peak power, 256 fs pulses was demonstrated by Haxsen et al. using a 2.8 m LMA fiber [7]. By increasing the stretched pulse duration to 160 ps, Sims et al. used a 3.3 m LMA fiber to achieve 1 μJ, 3 MW peak power pulses [8]. Hoogland et al. demonstrated a compact CPA system, which generated pulses with 1 MW peak power and 371 fs duration with a 3.4 m LMA fiber amplifier [9]. All these silica fiber based results required active fiber lengths above 1 m, which resulted in limited pulse-energy/peak-power scaling due to the appearance of detrimental nonlinear effects including modulation instability and spectral broadening from self-phase modulation (SPM).

Although silica glass is clearly both the dominant and most technologically developed host material for fiber lasers, due largely to its combination of favorable mechanical and glass-drawing characteristics, it has low rare-earth ion solubility, which limits the scope for reducing the lengths of active fiber in lasers and amplifiers. The maximum Tm³⁺ doping concentration in pure silica fiber is 10¹⁸ - 10¹⁹ ions/cm³ [10]. Higher doping levels (10²⁰ ions/cm³) can be realized through the addition of co-dopants such as aluminum or phosphorous [11], but these substantially increase the core refractive index relative to a pure-silica cladding, so cores with a surrounding pedestal structure are required to create the low index step needed in LMA designs. The need for this refractive index pedestal makes fabrication more complex. In contrast, heavy metal oxide glasses such as germanate and fluoride have much higher Tm³⁺ solubility with concentrations of 10²¹ ions/cm³ being readily achievable without the addition of co-dopants. The resulting promise of shorter device lengths should reduce the impact of

detrimental nonlinearities in pulsed laser systems. Germanate and fluoride glasses systems can be easily and directly index-matched to pure cladding glasses enabling simplified LMA step-index fiber design and fabrication. Here we focus on germanate glass, which has a nonlinear index approximately twice that of pure silica, so a reduction in device length by approximately that factor is required to compete with silica devices.

The other concern with silica glass is its high phonon energy of $\sim 1100 \text{ cm}^{-1}$, which results in fast multiphonon relaxation in the mid-IR, where it becomes opaque, and can also lead to a low cross-relaxation rate and thus reduction in quantum efficiency when pumping thulium at 793 nm [12-14]. In contrast, germanate glasses [15] possess a 25% lower phonon energy of $\sim 845 \text{ cm}^{-1}$ [16]. Hence, germanate fiber is attractive for laser transitions at long wavelengths that would not be useable in a silica glass host fiber. The outstanding challenges for realizing practical germanate fibers are in the fabrication of a glass with the lowest possible levels of impurities and in the preparation of a preform and fiber that do not suffer from crystallization so as to minimize propagation losses and achieve optimal laser performance.

Some good laser results with germanate fibers have already been achieved. Wen et al. demonstrated a single-frequency fiber laser at 1.95 μm using just 1.6 cm of a highly Tm doped ($7.6 \times 10^{20} \text{ ions/cm}^3$) barium gallo-germanate (BGG) single mode (SM) fiber but with a low output power (35 mW) and even moving to a length of 10 cm for multi-longitudinal-mode laser operation only 165 mW of output power was achieved with a moderate slope efficiency (17%) [16]. Fang et al. demonstrated a nanosecond-pulsed 2 μm single frequency master oscillator power amplifier (MOPA) using 41 cm of large core (30 μm) Tm-doped germanate fiber, obtaining a record output average power of 16 W and peak power of 73 kW [17]. However, their amplification slope efficiency of 17% was again low due to a high background loss of 5 dB/m in their fiber.

In this letter, we demonstrate a Tm doped germanate fiber with high dopant concentration, low background loss and a hexagonal cladding structure which enables efficient high-power cladding pumping. To highlight the opportunities this presents for laser development, we incorporated 65 cm of fiber, cladding pumped, in a compact, high average- and peak-power CPA system operating at 1925 nm, achieving 310 fs compressed pulses at an average power of 14.1 W and a peak power of 2.17 MW at a repetition rate of 15.7 MHz. By core pumping 19 cm of the same fiber and reducing the pulse repetition rate to 0.39 MHz we generated 290 fs pulses at average power of 2.3 W and peak power of 16 MW.

For the TDGF development, the germanate core glass (Ge-01) and cladding glass (Ge-02) were both made in house, using the melt-quenching technique from the chemical composition of $58\text{GeO}_2\text{-}15\text{PbO}\text{-}13\text{ZnO}\text{-}4\text{Nb}_2\text{O}_5\text{-}7\text{Na}_2\text{O}\text{-}1.5\text{SiO}_2\text{-}1.5\text{Al}_2\text{O}_3$ [18].

The combination provided the low refractive index contrast necessary for single mode LMA fiber operation and compatibility in terms of the thermo mechanical properties needed for successful fiber drawing. We achieved a high Tm^{3+} concentration of $3 \times 10^{20} \text{ ions/cm}^3$, a large core diameter of 20 μm and low numerical aperture ($\text{NA} = 0.07$) which, together, enabled robust SM operation. The fabrication process for the germanate glasses and TDGF were similar to the process as described in our report of a TDGF with a circular inner-cladding [18]. The Ge-01 cane and Ge-02 hexagonal glass tube were co-drawn into an optical fiber using a rod-in-tube technique (Fig. 1 left). The fiber core and cladding diameters were $20 \pm 0.5 \mu\text{m}$ and $126 \pm 1 \mu\text{m}$ (across 2 opposite angles), respectively.

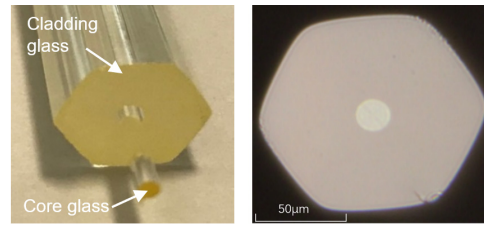


Fig. 1. (left) Cross sectional view of the extruded hexagonal inner cladding with the core rod extending outwards from the front face. (right) Optical microscope image of the fabricated Tm doped germanate LMA single mode fiber.

As shown in Fig. 1 right, there are no signs of residual stresses or bubbles at the interface between the core and cladding, which demonstrates the excellent quality of the drawing process. A UV curable low index acrylate polymer coating around the hexagonal cladding was added to provide mechanical protection and to allow the fiber to be cladding pumped by confining the pump power in the inner cladding. The fiber propagation loss was measured to be $\sim 1 \text{ dB/m}$ at 980 nm using the cut-back method, matching the lowest loss achieved for germanate glass fiber we reported earlier [17] and confirming the good reproducibility we have achieved in fabricating the high quality germanate glass material, and the excellent control we have of the fiber fabrication process.

The cladding pumped CPA system is illustrated schematically in Fig. 2. It comprises a fiber oscillator, fiber stretcher, two amplifier stages and a bulk grating based compressor. The dissipative soliton fiber oscillator has been described previously [19] and it provides chirped laser output pulses with a width of 25 ps, at a central wavelength of 1925 nm (39 nm bandwidth) at a repetition rate of 15.7 MHz. The average power output power was 40 mW (corresponding to a pulse peak power of 102 W). The pulses were then attenuated to 3 mW average power to minimize nonlinearity in the stretcher, which consisted of 58 m of UHNA7 (Nufern) and 25 m of UHNA4 (Nufern) fibers. This combination of fiber lengths was chosen to cancel the overall third order dispersion and to produce stretched pulses with duration of 140 ps [20]. These were amplified to an average power of 150 mW in a 1.5 m Tm-doped silica fiber (OFS, TmDF200) which was backward core-pumped with power of 400 mW at 1560 nm so as to minimize the effective nonlinear length.

To obtain the single polarization required for our transmission grating-based compressor, we used a polarization maintaining (PM) fast-axis blocking isolator preceded by an in-line polarization controller (FIBERPRO PC1100) between the pre- and power-amplifier stages. Due to slight depolarization in the fiber stretcher the power reduced from 150 mW to 110 mW even after precise adjustment of the PC. The final power amplifier comprised 65 cm of TDGF which was cladding pumped by two 30 W multimode-diodes (BWT) at 793 nm through a fiberized 130 μm cladding-diameter silica fiber-based combiner (Lightcomm) with a 10 μm core-throughput. The cladding absorption was 20 dB/m at 793 nm and the TDGF length was chosen to obtain a suitably centered spectral gain profile and a good amplifier efficiency. The mode field diameter of the TDGF at 1925 nm was 22.6 μm . The measured splicing losses between the TDGF and the combiner fiber where $< 1.2 \text{ dB}$ (due to the mode field diameter mismatch) and 0.2 dB, respectively, for the core and cladding.

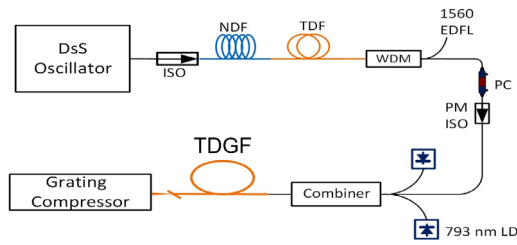


Fig. 2. Schematic diagram of the CPA system. DsS-dissipative soliton, NDF-normal dispersion fiber, WDM-wavelength-division multiplexer, PC-polarization controller, EDFL-Er doped fiber laser.

An offset-arc splicing technique (i.e. offsetting the arc position from the splicing location) was used because the germanate fiber has a lower melting temperature than silica glass [21]. The splice was re-coated with low index polymer and the TDGF was mounted onto a water-cooled plate and graphite sheets were applied to assist in the overall thermal management.

Although the available pump power was 60 W, the TDGF fiber damaged (inside the fiber and close to the input facet) at pump powers above 53 W (we observed this on 5 separate occasions at the ~50 W power level). We also observed the same effect when the pulsed seed was replaced with a cw-seed laser. In order to analyze the heat load of the TDGF, the temperature distribution of our fiber (fiber length=65 cm) was simulated using COMSOL Multiphysics at cladding pump power of 50 W. The fiber coating temperature reaches almost 100 oC. Consequently, we conclude that the damage we observed experimentally was due to thermal damage. We estimate that it may be possible to further increase the pump power by a factor of 4 or so based on the improved cooling arrangements and metal coating approach described in [22], but as of yet we have not investigated this. The maximum amplifier output was consequently limited to 20 W and the launched pump slope efficiency was 38.7% (see Fig. 3 (a)), well above the 32% we achieved using a commercial Tm-doped silica fiber in earlier work in the same basic set up [19]. No degradation in output power was observed over the >20 hours of total use of our CPA system, implying that photodarkening is not an issue in our fibers. To validate this more carefully, we undertook a more systematic experiment in which we incorporated a length of fresh fiber in our amplifier and seeded it with cw-laser light at 1953 nm. The amplifier was operated at our maximum pump power of 50 W and the amplified output power was measured every 30 s for a period of 6 hours from first turn on. As shown in Fig. 3(b), no degradation in output power was observed over the duration of our experiment confirming that photodarkening is not an issue on this fiber in agreement with our CPA system observations. The output beam quality was also measured at the maximum output power of 14.1 W (after the compressor) and high beam quality factor ($M^2 \sim 1.1$) was confirmed. The output spectrum is shown in Fig. 4(a).

The pulses were then recompressed using a pair of fused silica transmission gratings (Ibsen Photonics A/S) with a single pass transmission efficiency of 94% in the 1900 nm-2100 nm range. The polarization of the pulses incident to the gratings was controlled using bulk waveplates at the fiber output (a maximum incident PER of 16 dB was achieved). The overall double-pass compressor throughput was 14.1 W (70.5% measured efficiency). With an appropriate grating separation, a minimum compressed pulse duration of 310 fs was achieved as measured with a SHG autocorrelator (APE Pulse-check) (see Fig. 4(b)). The estimated

time bandwidth product (TBP) of 0.98 is 2.2 times the transform-limited value for a Gaussian pulse (0.44), but close to that of a transform-limited pulse with a rectangular-spectrum (0.88).

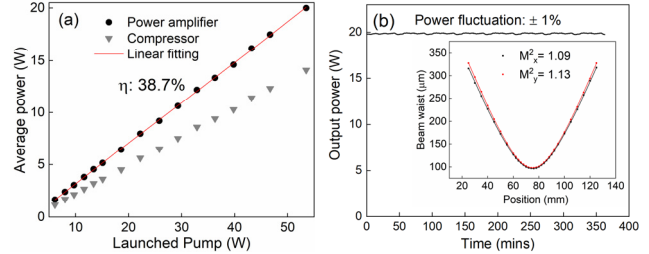


Fig. 3. (a) Measured average output power after the cladding-pumped power amplifier and compressor gratings versus launched pump power. (b) Long term stability test at the highest output power and the measured M^2 value ($M^2 \sim 1.1$).

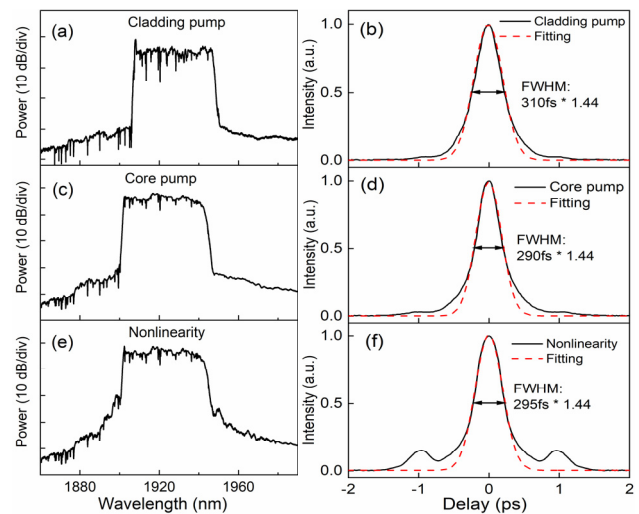


Fig. 4. Output spectra from the power amplifier and autocorrelation traces after the compressor. (a) and (c), Spectra at the maximum amplifier output power of 20 W and 3.2 W for cladding pumping and core pumping respectively. (b) and (d), Autocorrelation trace at the maximum output power of 14.1 W and 2.3 W after the compressor for cladding pumping and core pumping respectively. (e) Spectrum at a higher amplifier output power of 3.6 W for core pumping. (f) Autocorrelation trace at an output power of 2.55 W after the compressor for core pumping illustrating the deleterious impact of nonlinearity in the final stage amplifier.

We calculated the Fourier transform of the spectrum and estimated that 75% of the energy was in the main peak yielding a peak power estimate of 2.17 MW. Note that the atmospheric gas absorption lines clearly observable in the spectra in Fig. 4 originate from free space propagation in the air within the compressor (path length = 2.4 m) and during measurement in the OSA (internal path length approximately 2.8 m). It has previously been demonstrated that such gas absorption lines can degrade the temporal quality of compressed pulses, resulting in the formation of extended pulse tails extending over a time frame of several picoseconds [23]. By calculating the Fourier transform of the measured pulse spectrum including the air absorption lines, and with those artificially removed numerically, we estimate that only 2% of the pulse energy

is shed into low level pulse tails in our experiments due to absorption in air. As shown in Fig. 3(b), the spatial mode out of the compressor was measured to have M_x^2 and M_y^2 of 1.09 and 1.13, respectively, indicating close-to pure-single-mode operation and confirming the desired fundamental mode guidance was achieved in the TDGF. We next investigated core pumping a shorter length of TDGF (19 cm) in the power amplifier for pulse energy and peak power scaling. A fiber coupled polarization dependent acousto-optic modulator (AOM) was inserted after the pre-amplifier to reduce the repetition rate from 15.7 MHz to 0.39 MHz. A 30 cm of PM Tm-doped fiber with a core diameter of 10 μm (Nufern) was core pumped at 1560 nm and added as an extra pre-amplifier to boost the power into the final amplifier from 0.8 mW to 40 mW.

The 19 cm TDGF final amplifier was core-pumped via a 1565 nm EDFL pump laser (SPI Lasers) having a maximum power of 10 W through a PM-WDM coupler (Lightcomm). The core splicing loss between the TDGF and pigtail fiber of the silica fiber based PM-WDM was similar to that of the cladding pumped case (<1.2 dB). Fig. 4(c) shows the signal spectrum at the maximum average output power of 3.2 W for an incident pump power of 9 W (measured immediately after the WDM), this is the highest output power achieved in germanate fibers using in-band core pumping (corresponding to a slope efficiency with respect to incident pump power of 36%). Accounting for a careful cut back measured splice loss of 1.2 dB for the launched pump in the core, the slope efficiency with respect to absorbed pump power was 48%, which is comparable to the value we reported previously [19]. The corresponding autocorrelation trace of the compressed pulse is shown in Fig. 4(d) and shows a pulse duration of 290 fs. The TBP of 0.94 is similar to the cladding pumped result. We calculated that 80% of the energy was in the body of the pulse, so at a recompressed average power of 2.3 W, the pulse energy was estimated to be 4.7 μJ and the peak power 16 MW. Excellent spatial mode quality was evidenced by the M_x^2 and M_y^2 values of 1.09 and 1.11 respectively.

The maximum pulse energy was limited in these experiments by the appearance of spectral wings induced by nonlinear effects as shown in Fig. 4(e) (data taken at an incident pump power of 10 W and an amplifier output power of 3.55 W). The corresponding compressed autocorrelation trace shown in Fig. 4(f) indicates the formation of significant satellite-pulses.

In conclusion, we have fabricated a highly doped Tm-doped germanate fiber with a hexagonal inner cladding for efficient cladding pumped amplifier. In-house glass melting, preform glass extrusion and fiber drawing were used to achieve a background loss of just 1 dB/m, matching our earlier result [18]. Cladding pumping of a 65 cm length of TDGF produced pulses with average power of 14.1 W and peak power of 2.17 MW at the output of our CPA system. Core pumping a 19 cm TDGF produced pulses with average power of 2.3 W and a peak power of 16 MW. The results are already comparable with our record peak/average powers from a very similar femtosecond conventional/flexible-fiber thulium doped silica fiber CPA system [19], which confirms that the highly Tm³⁺-doped germanate glass single mode fiber can be an alternative to silica based fiber for 2 μm high energy/peak power pulses generation. Given the rapid ongoing progress in our fiber development processes this fiber technology should ultimately be capable of achieving higher peak powers and similar or possibly even higher average powers in the future. Thus, the next step in our research is to optimize the fiber fabrication to enable greater power

scaling. In parallel we will explore the possibility of further peak-power scaling by shortening the fiber length with a newly developed LMA germanate glass fiber with higher Tm³⁺ doping concentration (8.5×10^{20} ions/cm³) for which the luminescence intensity reaches its maximum at 1.8 μm [24].

Funding. Engineering and Physical Sciences Research Council (EP/P030181/1, EP/P027644/1, EP/P012248/1), ERC project Lightpipe (grant agreement n° 682724)

Acknowledgments. Data published in this paper are available from the University of Southampton repository at <http://doi.org/10.5258/SOTON/XXXXX>. Zhengqi Ren thanks the China Scholarship Council for financial support of his PhD.

Disclosures. The authors declare no conflicts of interest.

References

- Q. Fu, L. Xu, S. Liang, D. P. Shepherd, D. J. Richardson and S. Alam, *IEEE J. Quantum Electron.* **24**, 1 (2018).
- M. P. Arpin, T. Popmintchev, M. Gerrity, B. Zhang, M. Seaberg, D. Popmintchev, M. M. Murnane, and H. C. Kapteyn, *Phys. Rev. Lett.* **105**, 173901 (2010).
- E. A. Peralta, K. Soong, R. J. England, E. R. Colby, Z. Wu, B. Montazeri, C. McGuinness, J. McNeur, K. J. Leedle, D. Walz, E. B. Sozer, B. Cowan, B. Schwartz, G. Travish, and R. L. Byer, *Nature* **503**, 91 (2013).
- C. Gaida, M. Gebhardt, T. Heuermann, F. Stutzki, C. Jauregui, and J. Limpert, *Opt. Lett.* **43**(23), 5853–5856 (2018).
- C. Gaida, M. Gebhardt, F. Stutzki, C. Jauregui, J. Limpert, and A. Tünnermann, *Opt. Lett.* **41**(17), 4130–4133 (2016).
- P. Wan, L.-M. Yang, and J. Liu, *Opt. Express* **21**, 21374–21379 (2013).
- F. Haxsen, D. Wandt, U. Morgner, J. Neumann, and D. Kracht, *Opt. Lett.* **35**, 2991 (2010).
- R. A. Sims, et al., *Opt. Lett.* **38**, 123 (2013).
- H. Hoogland and R. Holzwarth, *Opt. Lett.* **40**, 3520 (2015).
- F. Auzel and P. Goldner, *Opt. Mater.* **16**, 93–103 (2001).
- R. Tumminelli, V. Petit, A. Carter, A. Hemming, N. Simakov, and J. Hob, *Proc. SPIE*, 105120M (2018).
- B. M. Walsh and N. P. Barnes, *Appl. Phys. B* **78**, 325–333 (2004).
- M. Eichhorn and S. D Jackson, *Appl. Phys. B* **90**, 35–41 (2008).
- S. D. Jackson, *Opt. Communications* **230**, 197–203 (2004).
- J. Wu, Z. Yao, J. Zong and S. Jiang, *Opt. Lett.* **32**, 638–640 (2007).
- X. Wen, G. Tang, Q. Yang, X. Chen, Q. Qian, Q. Zhang, and Z. Yang, *Sci. Rep.* **6**, 20344 (2016).
- Q. Fang, W. Shi, K. Kieu, E. Petersen, A. Chavez-Pirson, and N. Peyghambarian, *Opt. Express* **20**, 16410–16420 (2012).
- F. B. Slimen, S. Chen, J. Lousteau, Y. Jung, N. White, S. Alam, D. J. Richardson, and F. Poletti, *Opt. Mater. Express* **9**, 4115 (2019).
- Z. Ren, Q. Fu, L. Xu, J. H. V. Price, S. Alam, and D. J. Richardson, *Opt. Express* **27**, 36741 (2019).
- P. Elahi, H. Kalaycıoğlu, Ö. Akçaalan, Ç. Şenel, and F. Ö. İlday, *Opt. Lett.* **42**, 3808 (2017)
- R. Thapa, R.R Gattas, V. Nguyen, G. Chin, D. Gibson, W. Kim, L.B. Shaw and J.S. Sanghera, *Opt. Lett.* **40**, 5074 (2015).
- J. Daniel, N. Simakov, A. Hemming, W. Clarkson, and J. Haub, *Opt. Express* **24**, 18592–18606 (2016).
- M. Gebhardt, C. Gaida, F. Stutzki, S. Hädrich, C. Jauregui, J. Limpert, and A. Tünnermann, *Opt. Express* **23**, 13776 (2015).
- F. B. Slimen, Z. Ren, A. Ventura, J. Grigoletto Hayashi, J. Cimek, N. White, Y. Jung, D. J. Richardson and F. Poletti, *Proc. SPIE* 11206, 1120609-1 (2019).

Full References

1. Q. Fu, L. Xu, S. Liang, D. P. Shepherd, D. J. Richardson and S. Alam, "Widely Tunable, Narrow-Linewidth, High-Peak-Power, Picosecond Midinfrared Optical Parametric Amplifier," *IEEE J. Quantum Electron.* **24**(5), 1-6 (2018).
2. M. P. Arpin, T. Popmintchev, M. Gerrity, B. Zhang, M. Seaberg, D. Popmintchev, M. M. Murnane, and H. C. Kapteyn, "Bright, coherent, ultrafast soft X-ray harmonics spanning the water window from a tabletop light source," *Phys. Rev. Lett.* **105**(17), 173901 (2010).
3. E. A. Peralta, K. Soong, R. J. England, E. R. Colby, Z. Wu, B. Montazeri, C. McGuinness, J. McNeur, K. J. Leedle, D. Walz, E. B. Sozer, B. Cowan, B. Schwartz, G. Travish, and R. L. Byer, "Demonstration of electron acceleration in a laser-driven dielectric microstructure," *Nature* **503**(7474), 91–94 (2013).
4. C. Gaida, M. Gebhardt, T. Heuermann, F. Stutzki, C. Jauregui, and J. Limpert, "Ultrafast thulium fiber laser system emitting more than 1 kW of average power", *Opt. Lett.* **43**(23), 5853-5856 (2018).
5. C. Gaida, M. Gebhardt, F. Stutzki, C. Jauregui, J. Limpert, and A. Tünnermann, "Thulium-doped fiber chirped-pulse amplification system with 2 GW of peak power," *Opt. Lett.* **41**(17), 4130–4133 (2016).
6. P. Wan, L.-M. Yang, and J. Liu, "High power 2 μm femtosecond fiber laser," *Opt. Express.* **21**, 21374–21379 (2013).
7. F. Haxsen, D. Wandt, U. Morgner, J. Neumann, and D. Kracht, "Pulse energy of 151 nJ from ultrafast thulium-doped chirped-pulse fiber amplifier," *Opt. Lett.* **35**(17), 2991-2993 (2010).
8. R. A. Sims, P. Kadwani, A. L. Shah and M. Richardson, "1 μJ , sub-500 fs chirped pulse amplification in a Tm-doped fiber system," *Opt. Lett.* **38**(2), 121-123 (2013).
9. H. Hoogland and R. Holzwarth, "Compact polarization-maintaining 2.05- μm fiber laser at 1-MHz and 1-MW peak power," *Opt. Lett.* **40**(15), 3520-3523 (2015).
10. F. Auzel and P. Goldner, "Towards rare-earth clustering control in doped glasses," *Opt. Mater.* **16**(1-2), 93–103 (2001).
11. R. Tuminelli, V. Petit, A. Carter, A. Hemming, N. Simakov, and J. Hob, "Highly doped and highly efficient Tm doped fiber laser," *Proc. SPIE* 10512, 105120M (2018).
12. B. M. Walsh and N. P. Barnes, "Comparison of Tm:ZBLAN and Tm:silica fiber lasers; Spectroscopy and tunable pulsed laser operation around 1.9 μm ," *Appl. Phys. B* **78**, 325–333 (2004).
13. Marc Eichhorn and S.D Jackson, "Comparative study of continuous wave Tm³⁺-doped silica and fluoride fiber lasers", *Appl. Phys. B* **90**, 35-41(2008).
14. [S.D. Jackson, "Cross relaxation and energy transfer upconversion processes relevant to the functioning of 2 \$\mu\text{m}\$ Tm³⁺-doped silica fibre lasers", *Opt. Communications.* **230**,197-203 \(2004\).](#)
15. J.Wu,Z.Yao, J.Zong and S.Jiang, "Highly efficient high-power thulium-doped germanate glass fiber laser," *Opt. Lett.* **32**, 638-640 (2007).
16. X. Wen, G. Tang, Q. Yang, X. Chen, Q. Qian, Q. Zhang, and Z. Yang, "Highly Tm³⁺ doped germanate glass and its single mode fiber for 2.0 μm laser," *Sci. Rep.* **6**(1), 20344 (2016).
17. Qiang Fang, Wei Shi, Khanh Kieu, Eliot Petersen, Arturo Chavez-Pirson, and Nasser Peyghambarian, "High power and high energy monolithic single frequency 2 μm nanosecond pulsed fiber laser by using large core Tm-doped germanate fibers: experiment and modeling," *Opt. Express* **20**(15), 16410-16420 (2012).
18. F. B. Slimen, S. Chen, J. Lousteau, Y. Jung, N. White, S. Alam, D. J. Richardson, and F. Poletti, "Highly efficient -Tm³⁺ doped germanate large mode area single mode fiber laser," *Opt. Mater. Express* **9**(10), 4115-4125 (2019).
19. Zhengqi Ren, Qiang Fu, Lin Xu, Jonathan H. V. Price, Shaif-ul Alam, and David J. Richardson, "Compact, high repetition rate, 4.2 MW peak power, 1925 nm, thulium-doped fiber chirped-pulse amplification system with dissipative soliton seed laser," *Opt. Express* **27**(25), 36741-36749 (2019).
20. P. Elahi, H. Kalaycıoğlu, Ö. Akçaalan, Ç. Şenel, and F. Ö. İlday, "Burst-mode thulium all-fiber laser delivering femtosecond pulses at a 1 GHz intra-burst repetition rate," *Opt. Lett.* **42**(19), 3808-3811 (2017).
21. [Rajesh Thapa, Rafael R. Gattass, Vinh Nguyen, Geoff Chin, Dan Gibson, WooHong Kim, L. Brandon Shaw, and Jasbinder S. Sanghera, "Low-loss, robust fusion splicing of silica to chalcogenide fiber for integrated mid-infrared laser technology development," *Opt. Lett.* **40**, 5074-5077 \(2015\).](#)
22. J. Daniel, N. Simakov, A. Hemming, W. Clarkson, and J. Haub, "Metal clad active fibres for power scaling and thermal management at kW power levels," *Opt. Express* **24**(16), 18592-18606 (2016).
23. M. Gebhardt, C. Gaida, F. Stutzki, S. Hädrich, C. Jauregui, J. Limpert, and A. Tünnermann, "Impact of atmospheric molecular absorption on the temporal and spatial evolution of ultrashort optical pulses," *Opt. Express* **23**, 13776 (2015).
24. F. Ben Slimen, Z. Ren, A. Ventura, J. Grigoletto Hayashi, J. Cimek, N. White, Y. Jung, D. J. Richardson and F. Poletti, "Highly Tm³⁺ doped germanate glass and associated double clad fiber for 2 μm lasers and amplifiers," *Proc. SPIE* 11206, 1120609-1 (2019).